Assembly of fibrillin microfibrils governs extracellular deposition of latent TGFβ

Teresa Massam-Wu*, Maybo Chiu*, Rawshan Choudhury, Shazia S. Chaudhry, Andrew K. Baldwin, Amanda McGovern, Clair Baldock, C. Adrian Shuttleworth and Cay M. Kielty‡

Wellcome Trust Centre for Cell-Matrix Research, Faculty of Life Sciences, University of Manchester, Manchester M13 9PT, UK

*These authors contributed equally to this work

‡Author for correspondence (cay.kielty@manchester.ac.uk)

Accepted 18 May 2010
Journal of Cell Science 123, 3006-3018

doi:10.1242/jcs.073437

Summary

Control of the bioavailability of the growth factor TGFβ is essential for tissue formation and homeostasis, yet precisely how latent TGFβ is incorporated into the extracellular matrix is unknown. Here, we show that deposition of a large latent TGFβ complex (LLC), which contains latent TGFβ-binding protein 1 (LTBP-1), is directly dependent on the pericellular assembly of fibrillin microfibrils, which interact with fibronectin during higher-order fibrillogenesis. LTBP-1 formed pericellular arrays that colocalized with microfibrils, whereas fibrillin knockdown inhibited fibrillar LTBP-1 and/or LLC deposition. Blocking α5β1 integrin or supplementing cultures with heparin, which both inhibited microfibril assembly, disrupted LTBP-1 deposition and enhanced Smad2 phosphorylation. Full-length LTBP-1 bound only weakly to N-terminal pro-fibrillin-1, but this association was strongly enhanced by heparin. The microfibril-associated glycoprotein MAGP-1 (MFAP-2) inhibited LTBP-1 binding to fibrillin-1 and stimulated Smad2 phosphorylation. By contrast, fibulin-4, which interacted strongly with full-length LTBP-1, did not induce Smad2 phosphorylation. Thus, LTBP-1 and/or LLC deposition is dependent on pericellular microfibril assembly and is governed by complex interactions between LTBP-1, heparan sulfate, fibrillin-1 and microfibril-associated molecules. In this way, microfibrils control TGFβ bioavailability.

Key words: Latent TGFβ-binding protein 1 (LTBP-1), Fibrillin-1, Microfibrils, MAGP-1, Heparin, Fibulin-4

Introduction

The bioavailability of TGFβ, a potent growth factor that profoundly influences numerous cellular processes, is tightly regulated in tissues, yet precisely how latent TGFβ is incorporated into the extracellular matrix is unknown. TGFβ is secreted from cells in its latent form, either as a small complex comprising TGFβ and its latency-associated propeptide (LAP) or as a larger complex (large latent complex; LLC), which comprises a latent TGFβ-binding protein (LTBP) disulfide-bonded to LAP (Hyytiäinen et al., 2004). LLC sequestration in the matrix is a poorly understood process. The contextual environment that facilitates this sequestration is proposed to depend on latent TGFβ-binding protein 1 (LTBP-1) association with fibronectin fibrils and their relocation to fibrillin microfibrils (Ramirez and Rifkin, 2009). The importance of microfibrils in TGFβ regulation is highlighted by pathologically elevated TGFβ activity in the connective-tissue disorder Marfan syndrome, which is caused by fibrillin-1 mutations that disrupt the formation and/or stability of tissues such as blood vessels, eyes and bones (Robinson et al., 2006). Mice depleted of fibulin-4, a microfibril-associated molecule, have elastic fibre defects (McLaughlin et al., 2006; Hanada et al., 2007; Horiguchi et al., 2009) and exhibit enhanced aortic TGFβ activity (Hanada et al., 2007). By contrast, mice lacking microfibril-associated glycoprotein MAGP-1 (also known as MFAP-2) have reduced TGFβ activity but no overt microfibril defects (Weinbaum et al., 2008). These phenotypes show that microfibrils govern TGFβ bioavailability.

Fibrillin microfibrils mainly comprise fibrillin-1 (Cain et al., 2006), although fibrillin-2 is incorporated during tissue development and remodelling (Ramirez and Sakai, 2010). LTBP-1 and fibrillins comprise repeating Ca^{2+}-binding epidermal-growth-factor-like domains (cbEGFs) interspersed with 8-cysteine-containing TGFβ-binding protein-like (TB) and hybrid domains (Hyytiäinen et al., 2004). LTBP-1 is probably not a structural component of microfibrils (Isogai et al., 2003; Cain et al., 2006), although LTBP-1 tissue distribution overlaps with, but is not identical to, that of fibrillin-1 (Raghunath et al., 1998; Dallas et al., 2000; Sinha et al., 2002; Isogai et al., 2003). The C-terminal region of LTBP-1 can interact with a four-domain N-terminal fibrillin-1 region, and with N-terminal fibrillin-2 with lower affinity, whereas fibulin-4 can inhibit the interaction of C-terminal LTBP-1 with fibrillin-1 (Isogai et al., 2003; Ono et al., 2009). Using rat osteosarcoma cells, Dallas et al. (Dallas et al., 2005) reported that fibrillin-1 is not required for LTBP-1 deposition. A study using neonatal fibroblasts indicated that LTBP-1 deposition depends on fibrillin-1 (Ono et al., 2009). However, fibrillin-1 might not be needed for LTBP-1 matrix deposition if fibrillin-2 is expressed (Vehviläinen et al., 2009).

It is now clear that the assembly of fibronectin and fibrillin-1 are interconnected. Similar to assembly of fibronectin, microfibril assembly requires α5β1 integrin (Kinsey et al., 2008), and fibronectin dimers further assemble into higher-order arrays through non-covalent associations with matrix, especially with fibrillin microfibrils (Ohashi and Erickson, 2009). In skin fibroblast cultures, assembly of fibrillin microfibrils is dependent upon fibronectin fibrillogenesis, and microfibrils colocalize with fibronectin during early matrix deposition in particular, whereas fibrillin-1 can also interact with fibronectin (Kinsey et al., 2008; Sabatier et al., 2009). LTBP-1 also colocalizes initially with fibronectin but subsequently adopts a distinct fibrillar arrangement (Taipale et al., 1996; Dallas et al., 2005). Interactions have been reported between fibronectin

and the N-terminal region of LTBP-1 by ELISA and blot overlay assays (Fontana et al., 2005). However, using solid-phase binding assays, no interactions of full-length LTBP-1 or LTBP-1 fragments with fibronectin were detected, except in the presence of heparin, which binds a hinge region of LTBP-1 (Chen et al., 2007).

In the extracellular matrix, N-terminal LTBP-1 becomes crosslinked by transglutaminases (Nunes et al., 1997; Verderio et al., 1999), which are enzymes that also act on fibrillin-1 (Qian and Glanville, 1997) and fibronectin (Telci and Griffin, 2006) and influence TGFβ expression and activity (Telci et al., 2009). In tissues, proteolysis of crosslinked LTBP-1 by enzymes such as BMP-1, MT1-MMP and plasmin are initiating events in TGFβ activation (Munger et al., 1997; Ge and Greenspan, 2006; Tatti et al., 2008). LTBP-1 can be dislodged from damaged microfibrils by fibrillin-1 fragments (Chaudhry et al., 2007).

Although it is known that newly secreted LLC binds to the extracellular matrix through LTBP-1 interactions, mechanisms underlying its incorporation into matrix are poorly understood. Indeed, it is not known whether LLC binds fibrillin and fibronectin, whether it binds fibrillin before, during or after microfibril assembly, or whether microfibril-associated molecules influence this association. We provide evidence that the deposition of LTBP-1-containing LLC is governed by pericellular assembly of fibrillin microfibrils through interactions with heparan sulfate and with microfibril-associated molecules that fine-tune TGFβ sequestration. MAGP-1 can inhibit LTBP-1 binding to fibrillin-1, whereas fibulin-4 binds LTBP-1 with high affinity, which suggests that it is a key mediator in the association of LTBP-1 with microfibrils. Thus, the cell-surface heparan-sulfate-rich microenvironment is an essential orchestrator of TGFβ sequestration within microfibrils, which also interact with fibronectin during higher-order fibrillogenesis.

Results

We have previously shown that TGFβ activity is enhanced when LTBP-1 is displaced from microfibrils by the fibrillin-1 fragment PF10 (Chaudhry et al., 2007). Here, using human dermal fibroblasts and pigmented retinal epithelial (ARPE-19) cells, which deposit microfibrils (Sato et al., 2007; Kinsey et al., 2008), and using human LTBP-1 and microfibrillar proteins (Fig. 1), we demonstrate that pericellular interactions with pro-fibrillin during microfibril deposition govern the extracellular deposition and storage of latent TGFβ, and thus TGFβ bioavailability, through interactions with heparin and/or heparan sulfate and microfibril-associated molecules.

LTBP-1 colocalizes with fibrillin and fibronectin during microfibril assembly

LTBP-1 and fibrillin-1 colocalize in some tissues (Raghunath et al., 1998; Dallas et al., 2000; Sinha et al., 2002; Isogai et al., 2003), whereas fibrillin-1 and fibronectin show colocalization in fibroblast cultures (Kinsey et al., 2008; Sabatier et al., 2009). Immunofluorescence analysis of adult human dermal fibroblasts from days 1-14 was conducted to compare the temporal and spatial colocalization of LTBP-1, fibrillin-1 and fibronectin during microfibril deposition (Fig. 2; and not shown). LTBP-1 was rapidly deposited and tightly colocalized with fibrillin-1. LTBP-1 and fibrillin-1 also showed colocalization with fibronectin.

ARPE-19 cells cultured for 14 days also deposited LTBP-1, which strongly colocalized with fibrillin-1 microfibrils (Fig. 3A). In stable fibrillin-1 knockdown cells, the presence of extracellular LTBP-1 was much reduced compared with wild-type cells, although weak LTBP-1 immunostaining was detected that colocalized with

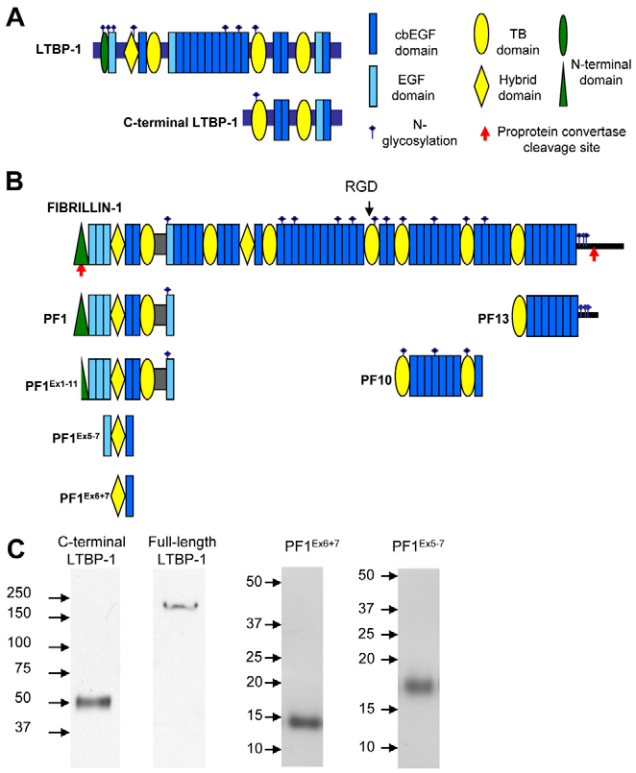

Fig. 1. Recombinant LTBP-1 and fibrillin-1. (**A**,**B**) Domain diagrams of (A) recombinant human full-length and C-terminal LTBP-1, and (B) recombinant human fibrillin-1 fragments, with domain key. (**C**) SDS-PAGE analysis, in the presence of 10 mM dithiothreitol, and of recombinant full-length LTBP-1, C-terminal LTBP-1, $PF1^{Ex6+7}$ or $PF1^{Ex5-7}$.

fibrillin-2 fibrils (Fig. 3A). Immunoblotting of medium and of cell-layer extracts from wild-type and knockdown cells (Fig, 3B) confirmed that the knockdown cells had no detectable fibrillin-1 in the medium and grossly reduced fibrillin-1 in the cell layer. LTBP-1 was present in the medium of both wild-type and knockdown cultures, but was markedly reduced in the knockdown cell layers, and LLC was undetectable. Thus, in these cultures, LTBP-1 deposition, but not its secretion, is governed by fibrillin-1. When fibrillin-1 or fibrillin-2 was depleted from human dermal fibroblasts using siRNA (not shown), LTBP-1 was still detected in fibrillar arrays. However, when both fibrillins were simultaneously depleted, LTBP-1 was present as a fine meshwork. Thus, both fibrillins can direct the fibrillar deposition of LTBP-1.

Disrupting microfibril assembly inhibits LTBP-1 deposition and activates TGFβ

Human dermal fibroblasts cultured for 5 days in the presence of anti-α5-integrin and anti-β1-integrin function-blocking monoclonal antibodies (mAb13, mAb16) have virtually no microfibril or fibronectin deposition; in these conditions, fibrillin-1 and fibronectin protein levels in medium and cell layers are unchanged (Kinsey et al., 2008). Here, the consequences for LTBP-1 deposition and TGFβ activity of blocking α5β1 integrin for 5 days were determined. Immunofluorescence analysis confirmed that there were virtually no microfibrils or extracellular LTBP-1 in these cultures (Fig. 4A). By contrast, cultures treated with a human-αv-integrin-blocking antibody (17E6) or αvβ3-integrin-blocking

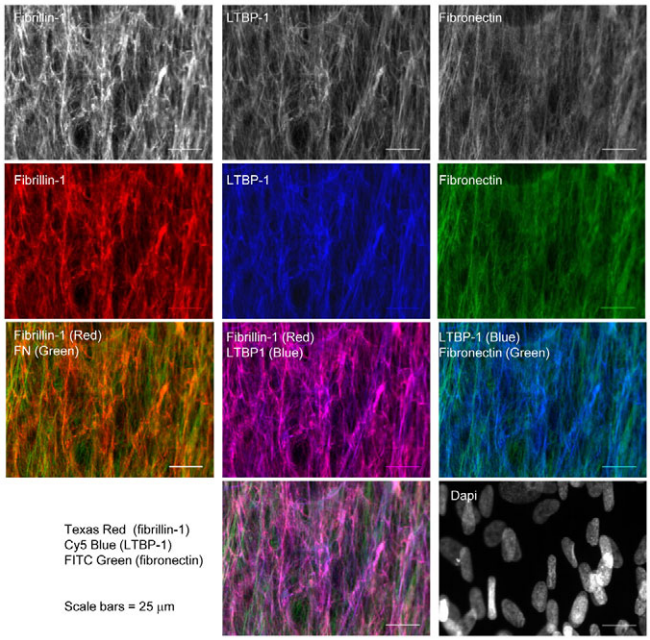

Fig. 2. Colocalization of LTBP-1 with fibrillin-1 in human dermal fibroblasts. Immunofluorescence microscopy of human dermal fibroblasts cultured for 14 days, showing deposition of fibrillin-1 (red), LTBP-1 (blue) and fibronectin (FN; green), with nuclei stained with DAPI (white). Images were taken on a wide-field upright microscope, using a 60× objective, and captured using a CoolSNAP EZ camera (Photometrics) driven by MetaVue Software (Molecular Devices). Specific band-pass filter sets for DAPI, FITC, Texas Red and Cy5 were used to prevent bleed-through. Images were processed and analyzed using ImageJ software. There was extensive colocalization of fibrillin-1 and LTBP-1 (to give purple), but only limited colocalization with fibronectin. Scale bars: 25 μm.

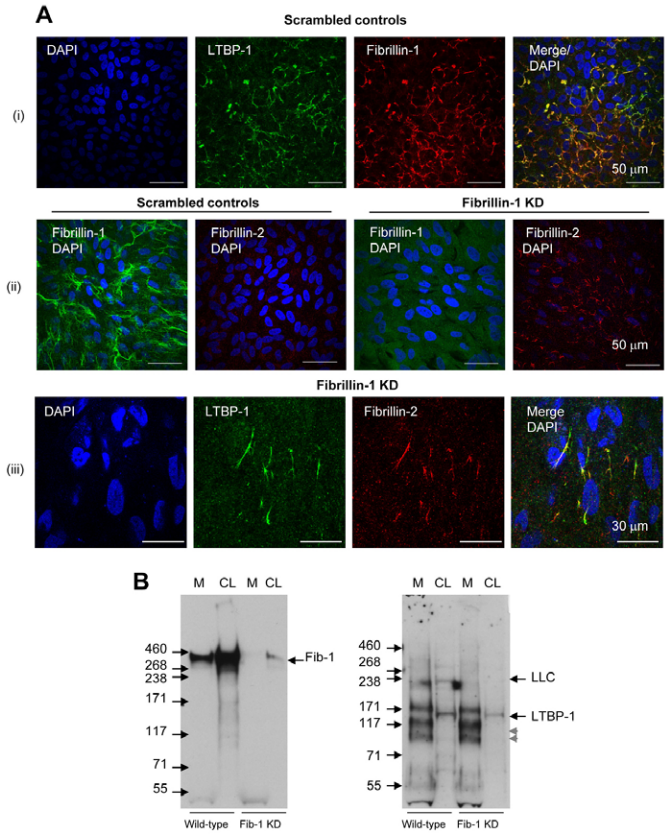

Fig. 3. Colocalization of LTBP-1 with fibrillin-1 in ARPE-19 cells. (**A**) Immunofluorescence microscopy of 'scrambled' control ARPE-19 cells and ARPE-19 cells with fibrillin-1 stably knocked down, after culture for 14 days, showing deposition of fibrillin-1 (proline-rich region antibody, red; mAb 11C1.3, green), or fibrillin-2 (red), LTBP-1 (green) and DAPI (blue). Images were collected using a Nikon C1 confocal on an upright 90i microscope with a 60×/1.40 Plan Apo objective. (i) LTBP-1 colocalized with fibrillin-1 in wild-type cells. (ii) Fibrillin-1 stable-knockdown cells, showing loss of fibrillin-1 microfibrils and appearance of low levels of fibrillin-2. (iii) Low levels of LTBP-1 and fibrillin-2 colocalized in fibrillin-1 knockdown cells. Scale bars: 50 μm. (**B**) SDS-PAGE and immunoblotting of fibrillin-1 and LTBP-1 in medium and in cell-layer extracts of wild-type and fibrillin-1 stable-knockdown ARPE-19 cells, after 5 days in culture. Fibrillin-1 was detected using a polyclonal antibody to the fibrillin-1 proline-rich region (Kinsey et al., 2008). Knockdown cells had no detectable fibrillin-1 in medium, and grossly reduced fibrillin-1 in the cell layer. LTBP-1 was detected using anti-LTBP-1 mAb 388 (Chen et al., 2007). LTBP-1 and LLC was present in medium and cell layer of control cultures. In fibrillin-1 knockdown cultures, LTBP-1 was detected in the medium, but the cell layer had reduced LTBP-1, and LLC was undetectable. Lower-M_r LTBP-1 bands (grey arrowheads) in medium (M) are proteolytic fragments (LTBP-1 is proteolytically cleaved upon release from matrix) (Dallas et al., 2002). Fib-1 KD, fibrillin-1 knockdown cells.

antibody (LM609) had abundant microfibrils with colocalizing LTBP-1 (Fig. 4A). Cultures treated with a β1-integrin-activating antibody (TS2/16) contained abundant microfibrils and LTBP-1 (Fig. 4A). We investigated whether α5β1-integrin blockade for 5 days altered TGFβ activity. Smad2 phosphorylation was significantly enhanced when α5β1 integrin was blocked (Fig. 4B) (Chaudhry et al., 2007). Thus, α5β1 integrin is necessary for LTBP-1 deposition and the stable storage of latent TGFβ.

Exogenous heparin blocks microfibril deposition (Tiedemann et al., 2001; Ritty et al., 2003), probably by disrupting fibrillin-1 self-association and interactions with syndecans, and impairs LTBP-1 incorporation into plasmin-solubilized matrix (Chen et al., 2007). Here, the consequences of exogenous heparin for LTBP-1 deposition and TGFβ activity were determined. In dermal fibroblasts supplemented for 5 days with heparin (0.5 mg/ml) (Tiedemann et al., 2001), LTBP-1 and microfibril deposition were both blocked (Fig. 5A). Fine punctate LTBP-1 filaments assembled on cell surfaces of untreated cultures, whereas filament assembly was grossly disrupted in heparin-treated cultures. In these conditions, fibrillin-1 and fibronectin protein levels in medium and in cell layers were unaltered, and heparin did not block fibronectin deposition (not shown) (Ritty et al., 2003; Chen et al., 2007). Immunoblotting of anti-LTBP-1-immunoprecipitated medium and in cell-layer extracts confirmed that exogenous heparin strongly inhibited LLC deposition (Fig. 5B).

Thus, the matrix association of LTBP-1-containing LLC, similar to microfibril assembly, requires α5β1 integrin and is disrupted by heparin.

Full-length LTBP-1 binds only weakly to fibrillin-1

Fibrillin-1 is secreted as an unprocessed pro-fibrillin-1 monomer and processed pericellularly by pro-protein convertases, as a prerequisite for assembly (Wallis et al., 2003). In vitro binding studies were conducted using full-length LTBP-1 with PF1 (Fig. 6A), or with deletion fragment $PF1^{Ex1\text{-}11}$, which lacks the 17 amino

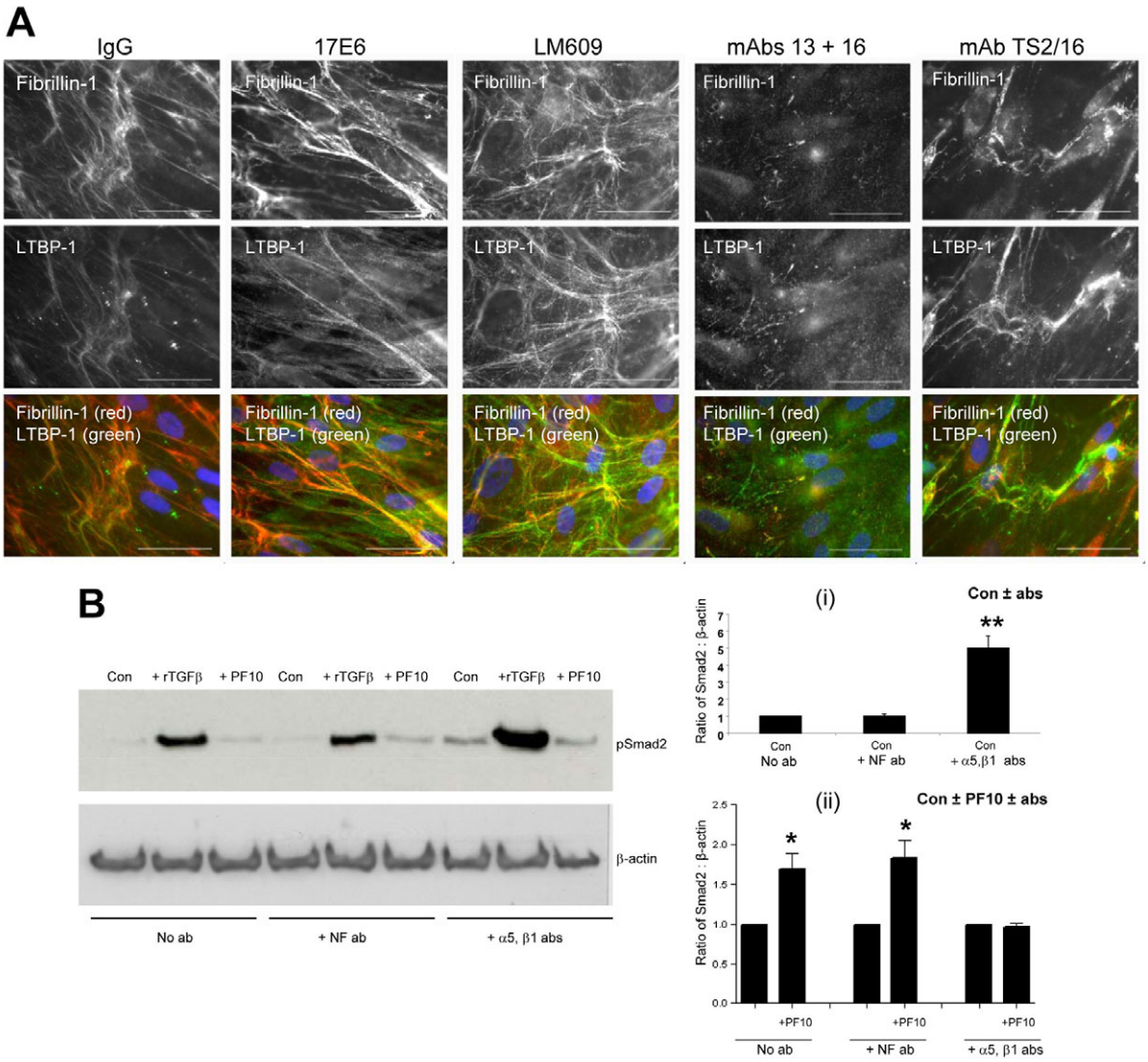

Fig. 4. Effects of integrin-modifying antibodies on LTBP-1 deposition. (**A**) Immunofluorescence microscopy of human dermal fibroblasts cultured for 5 days in the presence of mAbs that block integrins αv (17E6), αvβ3 (LM609) and α5β1 (mAbs 13, 16), or activate β1 integrins (TS2/16), showing effects on deposition of fibrillin-1 (red) and LTBP-1 (green), with DAPI-stained nuclei (blue). Control cells were incubated with mouse IgG (Kinsey et al., 2008) or with non-function-blocking antibody (mAb 11) (not shown). Images were taken on a wide-field upright microscope (Olympus BX51), using 60× objectives, and captured using a CoolSNAP EZ camera (Photometrics) driven by MetaVue Software (Molecular Devices). Specific band-pass filter sets for DAPI, FITC and Texas Red were used to prevent bleed-through. Images were processed and analyzed using ImageJ software. The α5β1, but not αv, integrin-blocking antibodies grossly inhibited fibrillin-1 and LTBP-1 deposition, whereas abundant fibrillin-1 and LTBP-1 were deposited in the presence of the β1-integrin-activating antibody. There was extensive colocalization of fibrillin-1 and LTBP-1. Scale bars: 50 µm. (**B**) Inhibiting α5β1 integrin enhanced Smad2 phosphorylation in human dermal fibroblasts. Thus, α5β1 is needed for the storage of latent TGFβ and, when blocked, there is significant release of endogenous TGFβ. When α5β1 had been blocked, the fibrillin-1 PF10 fragment that releases TGFβ from microfibrils (Chaudhry et al., 2007) could not release further TGFβ. Quantitative analysis was undertaken using densitometry, with data normalized against β-actin. Error bars represent the s.d. of two experiments. 'Con' shows fibroblasts cultured for 5 days in the absence of antibodies (no ab), or in the presence of α5-integrin non-function-blocking mAb 11 at 20 µg/ml (+NF ab), or in the presence of α5- and β1-integrin-blocking mAbs 13 and 16, both at 20 µg/ml (+α5, β1 abs). '+PF10' shows fibroblasts cultured for 5 days with 3 µM exogenous recombinant fibrillin-1 PF10 fragment that releases TGFβ from microfibrils (Chaudhry et al., 2007) (see also Fig. 8C). Fibroblasts were cultured in the presence of PF10 but no antibody (no ab), or in the presence of PF10 plus non-function-blocking mAb 11 (+NF ab), or in the presence of PF10 plus α5 and β1 integrin blocking mAbs 13 and 16 (+α5, β1 abs). '+rTGFβ' shows positive controls for TGFβ receptor-mediated phospho-Smad2 activity, induced by exogenous recombinant human TGFβ1 (4 nM), as shown by Chaudhry et al. (Chaudhry et al., 2007). Fibroblasts were cultured in the presence of rTGFβ but no antibody (no ab), or in the presence of rTGFβ plus non-function-blocking mAb 11 (+NF ab), or in the presence of rTGF plus α5- and β1-integrin -blocking mAbs 13 and 16 (+α5, β1 abs). When α5- and β1-integrin subunits were blocked, TGFβ-induced Smad2 signalling was enhanced. Graph (i): the 'Con +α5, β1 abs' sample had significantly enhanced Smad2 phosphorylation compared with 'Con, no abs' and 'Con +NF ab' samples. $^{**}P<0.001$ in comparison to '+NF ab', and $^{**}P<0.001$ in comparison to 'no ab', using one-way ANOVA followed by the Tukey's post-hoc test. Graph (ii): the '+PF10 no ab' and the '+PF10 +NF ab' samples both had significantly enhanced Smad2 phosphorylation compared with cells cultured without PF10. $^{*}P<0.05$ in comparison to no added PF10, using a one way ANOVA followed by the Tukey's post-hoc test. However, fibroblasts cultured in the presence of PF10 plus α5- and β1-integrin-blocking mAbs 13 and 16 ('+PF1 +α5, β1 abs') showed no significant difference from no added PF10. Each +PF10 test sample was compared with its relevant control, for which the ratio of phospho-Smad2:β-actin was set to 1.

acids (AGNVKETRASRAKR) that are removed by pro-protein convertase processing, or subfragment PF1^{Ex5-7} (not shown). BIAcore analysis showed that full-length LTBP-1 bound only very weakly to PF1, with a dissociation constant (K_D) of 1270±186 nM, and a K_D of 927.5±168.5 nM and 2016±45 nM for PF1^{Ex1-11} and PF1^{Ex5-7}, respectively. Thus, although some fibrillin-1 can co-immunoprecipitate with LTBP-1 (see Fig. 6D), full-length LTBP-1 only binds weakly to fibrillin-1.

C-terminal LTBP-1 was reported to bind within four N-terminal fibrillin-1 domains encoded by exons 4-7 (EGF2, EGF3, first hybrid and cbEGF1), and deletion or disruption of the first hybrid domain reduces affinity for LTBP-1 (Isogai et al., 2003; Ono et al., 2009). We have compared binding of fibrillin-1 to full-length and C-terminal LTBP-1. First, BIAcore analysis was used to analyze the C-terminal LTBP-1 interaction with fibrillin-1, with LTBP-1 immobilized on a CM5 chip (Fig. 6Bi-iii). PF1, the unprocessed N-terminal region of fibrillin-1 (Fig. 1A), bound to C-terminal LTBP-1 with moderate affinity (K_D=134.4±36.9 nM). PF1 subfragments encoded by fibrillin-1 exons 5-7 (designated PF1^{Ex5-7}; EGF3, first hybrid and cbEGF1) and exons 6-7 (designated

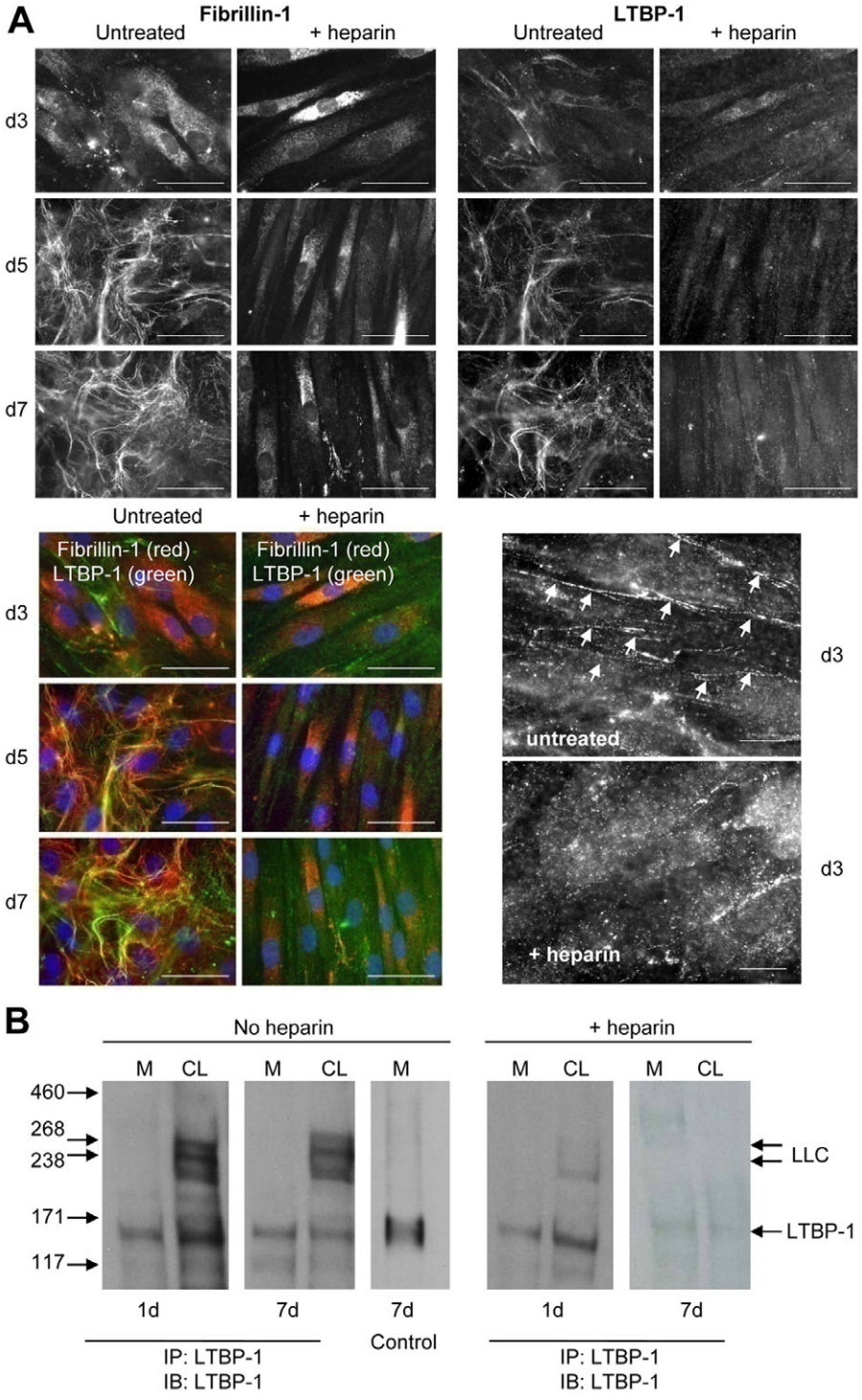

Fig. 5. Effects of heparin on LTBP-1 deposition. (**A**) Immunofluorescence microscopy of human dermal fibroblasts cultured for 5 days in the presence or absence of heparin (0.5 mg/ml), showing effects on deposition of fibrillin-1 (red) and LTBP-1 (green), with nuclei stained with DAPI (blue). Images were taken on a wide-field upright microscope (Olympus BX51), using 60× objective, and captured using a CoolSNAP EZ camera (Photometrics) driven by MetaVue Software (Molecular Devices). Specific band-pass filter sets for DAPI, FITC and Texas Red were used to prevent bleed-through. Images were processed and analyzed using ImageJ software. The heparin-treated cultures did not deposit either fibrillin-1 microfibrils or LTBP-1. Scale bars: 50 µm. In these conditions, fibronectin was assembled (not shown) (Ritty et al., 2003). Also shown are enlarged images (60× objective, as above) of untreated and heparin-treated fibroblasts (day 3), immunostained with anti-LTBP-1 antibody (mAb 388) and secondary Alexa-Fluor-488-conjugated antibody. Only untreated cultures show pericellular arrays of LTBP-1 (arrows). Scale bars: 25 µm. (**B**) Human dermal fibroblasts were cultured for up to 7 days ± heparin (0.5 mg/ml). Medium and cell-layers extract were immunoprecipitated with anti-LTBP-1 mAb388, and analyzed by SDS-PAGE and immunoblotting using the same anti-LTBP-1 antibody. In the absence of heparin, LTBP-1 appeared as a band at ~170 kDa in medium and cell layers, and LLC (230-270 kDa) (Miyazono et al., 1991; Taipale et al., 1996) was also present in cell layers. In the presence of heparin, the levels of LTBP-1 and LLC were grossly reduced at day 1 and virtually undetectable at day 7.

PF1^{Ex6+7}; first hybrid and cbEGF1) both bound more strongly than PF1 to C-terminal LTBP-1, with a K_D of 9.3±3.3 nM and 31.2 nm, respectively. Thus, C-terminal LTBP-1 binding to fibrillin-1 requires the first hybrid domain and cbEGF1. Because PF1 subfragments bind more strongly to C-terminal LTBP-1 than does PF1, the conformation of N-terminal fibrillin-1 must be crucial.

The fibrillin-1 mutation C166S causes classic Marfan syndrome with severe vascular pathology (Biggin et al., 2004), whereas the adjacent Marfan N164S mutation (Comeglio et al., 2002) causes a milder ocular and/or skeletal phenotype. Ono et al. showed that N164S, which is in the EGF domain that precedes the first hybrid domain, did not inhibit binding to C-terminal LTBP-1 (Ono et al., 2009). Here, mutation C166S significantly inhibited LTBP-1 binding (Fig. 6C), confirming that the EGF3 domain, which precedes the first hybrid domain, influences LTBP-1 binding.

Interactions between the N- and C-termini of different fibrillin-1 molecules stabilize its linear and lateral accretion (Marson et al., 2005; Hubmacher et al., 2008). We investigated whether the association of LTBP-1 with PF1 altered the ability of PF1 to participate in N-N- or N-C-terminal interactions, and thus microfibril assembly. We used solid-phase assays because fibrillin-1 binds poorly to BIAcore chips (Choudhury et al., 2009). In the presence of C-terminal LTBP-1, PF1 underwent N-N- and N-C-terminal interactions (not shown), so C-terminal LTBP-1 does not disrupt microfibril elaboration.

Because C-terminal LTBP-1 binds N-terminal fibrillin-1, and LTBP-1 colocalizes with fibrillin-1 and requires microfibril assembly for extracellular deposition, we investigated whether they directly associate. Using dermal fibroblasts cultured for up to 7 days, some fibrillin-1 co-immunoprecipitated with LTBP-1 in cell lysates (Fig. 6D). Thus, LTBP-1 and fibrillin-1 can associate during microfibril assembly.

Binding of full-length LTBP-1 to pro-fibrillin-1 is facilitated by heparin and/or heparan sulfate

We have shown that unprocessed N-terminal fibrillin-1 fragment PF1 interacts with cells in a heparan-sulfate-dependent manner (Bax et al., 2007), whereas heparin induces a very high heparin-

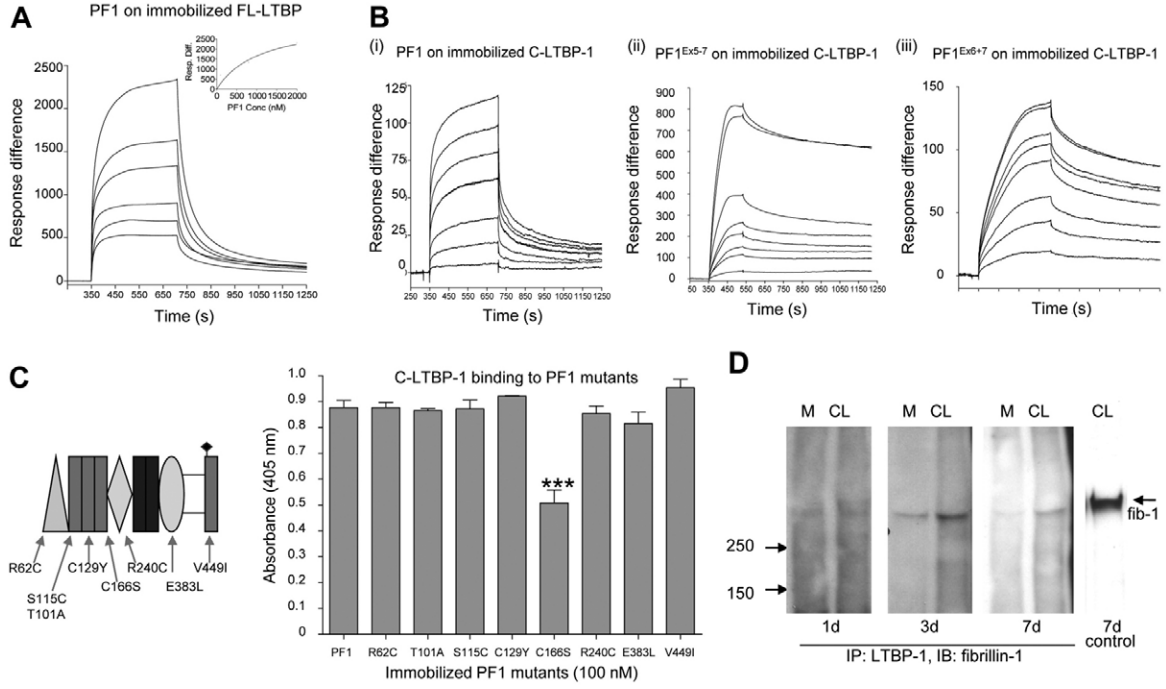

Fig. 6. LTBP-1 interactions with fibrillin-1. (**A**) BIAcore analysis of the binding of immobilized full-length LTBP-1 to PF1, the unprocessed N-terminal fibrillin-1 fragment (Cain et al., 2008). The sensorgram (inset) shows analyte concentrations ranging from 0-2000 nM, with duplicate concentrations in every run. One representative experiment is shown. Response difference is the difference between experimental and control flow cells, in response units. Time is shown in seconds. Evaluation of the kinetics of the interactions was performed according to a 1:1 Langmuir binding model. PF1 bound only weakly to full-length LTBP-1 (K_D=1270±186 nM). Data are mean ± s.e.m. of at least two separate experiments. Similarly, PF1^{Ex1-11} and PF1^{Ex5-7} showed only weak binding to full-length LTBP-1 (not shown). (**B**) BIAcore analysis of the binding of C-terminal LTBP-1 (C-LTBP-1), immobilized on a CM5 chip, to PF1 (i), PF1^{Ex5-7} (ii) or PF1^{Ex6+7} (iii). Sensorgrams show analyte concentrations ranging from 0-3000 nM, with duplicate concentrations in every run. One representative experiment is shown in each case. Response difference is the difference between experimental and control flow cells, in response units. Time is shown in seconds. Evaluation of the kinetics of the interactions was performed according to a 1:1 Langmuir binding model. Data are mean ± s.e.m. of at least two separate experiments. PF1 bound with moderate affinity to C-LTBP-1 (K_D=134.4±36.9 nM), whereas PF1^{Ex5-7} and PF1^{Ex6+7} bound strongly to C-LTBP-1 (K_D values=9.3±3.3 nM and 31.2±0 nM, respectively). (**C**) Solid-phase binding assays showing soluble biotinylated C-terminal LTBP-1 (C-LTBP-1) binding to immobilized wild-type PF1 or to eight N-terminal Marfan syndrome mutants (shown on the left). PF1 mutants were immobilized onto Immulon-4 HBX microtitre plates at 100 nM, and soluble biotinylated C-LTBP-1 was plated at 100 nM and detected at 405 nm. GraphPad Prism 4.0 was used to calculate significance using unpaired Student's *t*-tests. One representative experiment is shown. Data are shown with the negative (biotinylated LTBP-1 only) control subtracted. Results are shown as the mean ± s.e.m. of triplicate values. Soluble biotinylated LTBP-1 bound strongly to PF1 and seven of the mutants, but binding to mutant C166S was significantly reduced (***P<0.0001 by Student's *t*-test in comparison with wild-type PF1). (**D**) Human dermal fibroblasts were cultured for up to 7 days. Medium and cell-layer extracts were immunoprecipitated with anti-LTBP-1 mAb388, and analyzed by SDS-PAGE and immunoblotting using anti-fibrillin-1 proline-region antibody. Fibrillin-1 was detected mainly in cell-layer immunoprecipitates, as a 350 kDa band.

binding response to PF1 but not to 'processed' fragment $PF1^{Ex1-11}$, indicating heparin-mediated multimerization (Cain et al., 2005; Cain et al., 2008). Heparin was also shown to bind an N-terminal hinge region in LTBP-1 (Chen et al., 2007). Here, BIAcore analysis revealed that full-length LTBP-1 bound to heparin with high affinity (K_D=10.5±5.5 nM) (Fig. 7A), but C-terminal LTBP-1 did not bind heparin (not shown).

Heparin stimulated the binding of unprocessed PF1 to immobilized full-length LTBP-1 (Fig. 7Bi). However, heparin inhibited $PF1^{Ex1-11}$ binding to full-length LTBP-1, which differs from PF1 only by absence of the short sequence preceding the processing site (Fig. 7Bii). Heparin also strongly inhibited the short internal fragment $PF1^{Ex5-7}$ binding to full-length LTBP-1 (not shown). In parallel experiments with heparin immobilized, full-

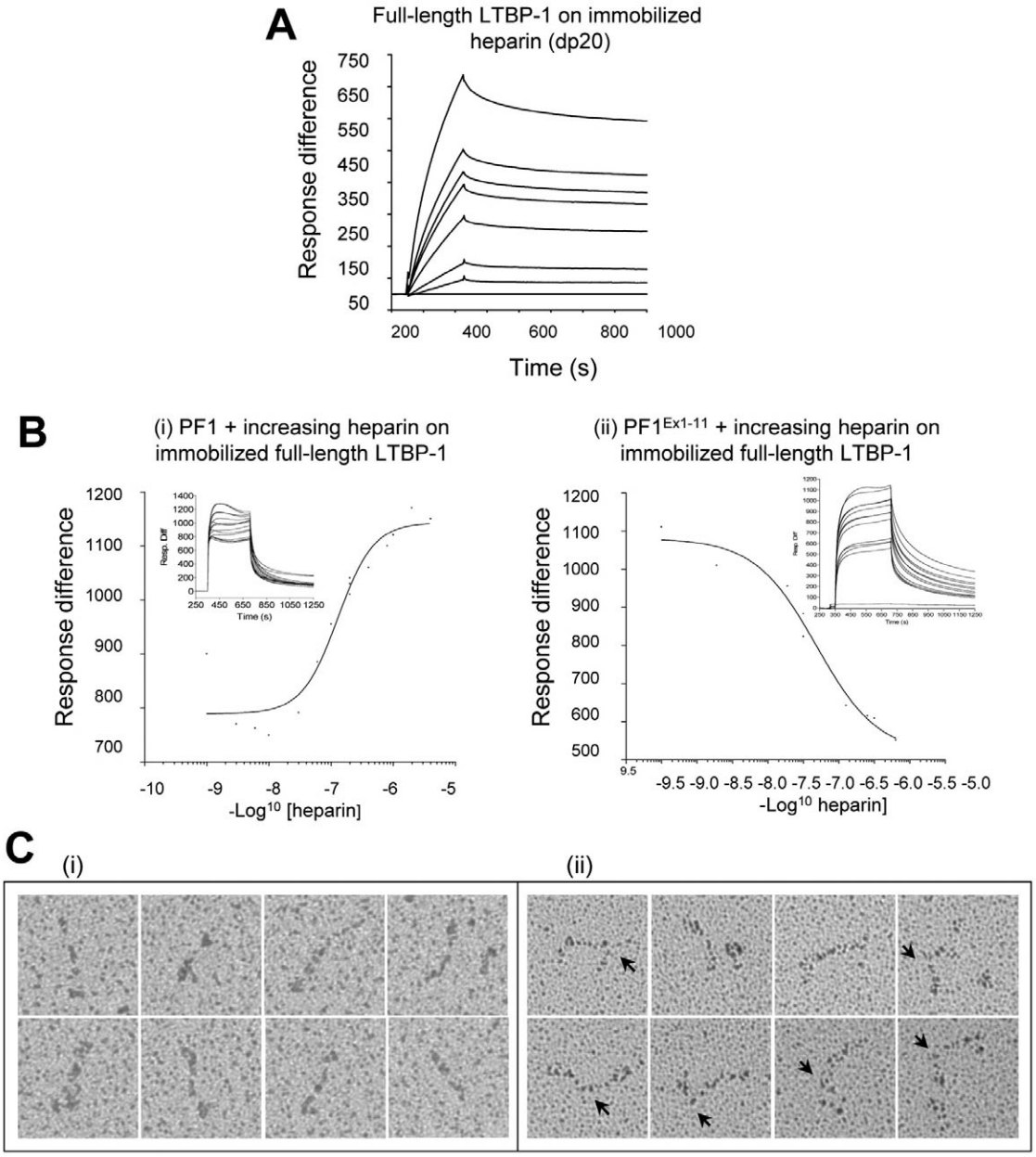

Fig. 7. Heparin enhances binding of full-length LTBP-1 to N-terminal pro-fibrillin-1. (**A**) BIAcore analysis of the binding of full-length LTBP-1 to heparin (dp20), which was immobilized on a streptavidin (SA) chip (Cain et al., 2005). The sensorgram shows full-length LTBP-1 analyte concentrations ranging from 0-200 nM, with duplicate concentrations included in every run. One representative experiment is shown. Response difference is the difference between experimental and control flow cells, in response units. Time is shown in seconds. Full-length LTBP-1 bound strongly to heparin (K_D=10.5±5.5 nM). (**B**) BIAcore analysis of the effects of heparin on the binding of N-terminal pro-fibrillin-1 (PF1) to full-length LTBP-1, which was immobilized on a CM5 chip. PF1 (200 nM) was injected after pre-incubation with 0-4000 nM heparin. (i) PF1 binding to full-length LTBP-1 is enhanced by heparin. However, (ii) $PF1^{Ex1-11}$ binding to full-length LTBP-1 is inhibited by heparin. At least two repeats of each experiment were conducted, and one representative experiment is shown. Response difference is the difference between experimental and control flow cells in response units. Inhibition curves were plotted using the response values of each normalized curve at the end of the association period. (**C**) Rotary shadowing of full-length LTBP-1 in the (i) absence or (ii) presence of heparin. In the absence of heparin, LTBP-1 had an average length of 68.2±2.3 nm (n=8), and in the presence of heparin it was 71.0±2.6 nm (n=8). The arrows in Cii indicate possible kinks. Each image represents 100×100 nm.

length LTBP-1 binding was stabilized by unprocessed PF1, but not by $PF1^{Ex1\text{-}11}$ or $PF1^{Ex4\text{-}11}$ (not shown). Thus, heparin-facilitated binding of LTBP-1 to fibrillin-1 requires both the heparin-binding N-terminal region of LTBP-1 and the heparin-multimerization motif of pro-fibrillin-1.

Rotary shadowing electron microscopy (EM) of purified full-length LTBP-1 (Fig. 7C) revealed rod-like molecules that were 68.2±2.3 nm in length in the absence of heparin, and 71.0±2.6 nm when pre-incubated with heparin. A number of molecules in the presence of heparin appeared bent.

LTBP-1–fibrillin-1 complexes are modulated by microfibril-associated molecules

We explored whether microfibril-associated molecules can also regulate the LTBP-1 interaction with fibrillin-1, and thus TGFβ bioavailability (Figs 8, 9).

Fibulin-4 binds strongly to full-length LTBP-1 and fibrillin-1

Fibulin-4 binds fibrillin-1 (Choudhury et al., 2009; Ono et al., 2009) and colocalizes with microfibrils (Kobayashi et al., 2007), and fibulin-4 hypomorphic mice have enhanced TGFβ activity (Hanada et al., 2007). Here, BIAcore analysis revealed that full-length LTBP-1 bound strongly to immobilized full-length fibulin-4 (K_D=2.1±0.12 nM) (Fig. 8Ai) and full-length fibulin-4 also bound strongly to immobilized full-length LTBP-1 (K_D=10.07±0.82 nM) (not shown). This fibulin-4 interaction is with the N-terminal half of LTBP-1 (not shown). We have previously shown that fibrillin-1 fragment PF1 also binds fibulin-4 (Choudhury et al., 2009); here we show that PF1 (200 nM) and full-length LTBP-1 (200 nM) can both simultaneously bind to immobilized full-length fibulin-4 (200 nM) (Fig. 8Aii).

Having shown that fibulin-4 can strongly bind LTBP-1, and can simultaneously bind LTBP-1 and fibrillin-1, we found that fibulin-

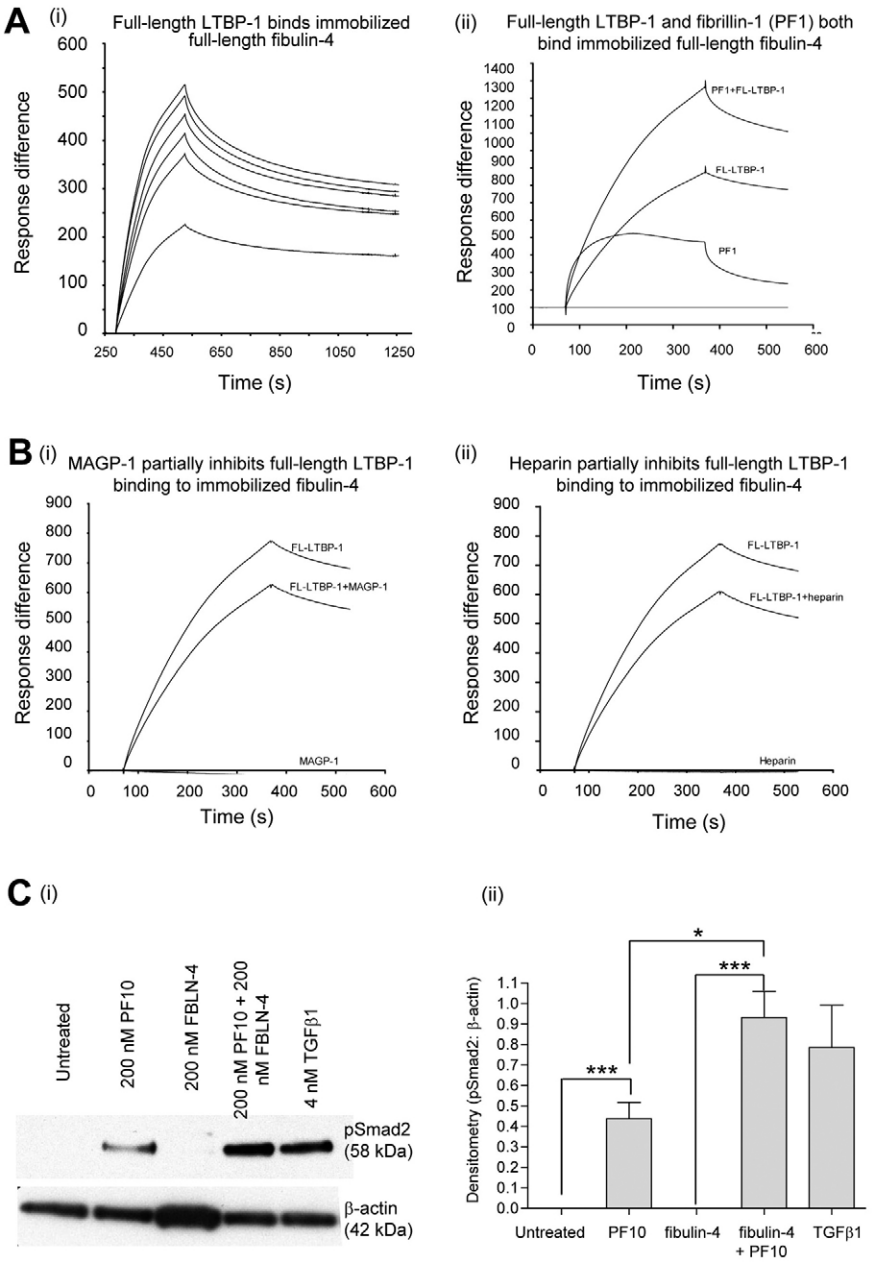

Fig. 8. Fibulin-4 forms a stable ternary complex with full-length LTBP-1 and fibrillin-1. BIAcore analysis revealed strong binding between full-length LTBP-1 and full-length fibulin-4, and that fibulin-4 forms a stable complex with LTBP-1 and fibrillin-1. (**A**) (i) Full-length LTBP-1 (FL-LTBP-1) (0-10 μg/ml) bound strongly to immobilized full-length fibulin-4 (K_D=2.1±0.12 nM). (ii) Full-length LTBP-1 (200 nM) bound strongly to immobilized full-length fibulin-4, concurrently with fibrillin-1 (PF1; 200 nM). (**B**) (i) Full-length LTBP-1 (FL-LTBP-1) (200 nM) binding to immobilized full-length fibulin-4 was partially inhibited by MAGP-1 (200 nM). (ii) Full-length LTBP-1 (200 nM) binding to immobilized full-length fibulin-4 was partially inhibited by heparin (3000 kDa; Sigma-Aldrich, UK) (200 nM). For A and B, duplicate concentrations were included in every run. One representative experiment is shown in each case. Response difference is the difference between experimental and control flow cells, in response units. Time is shown in seconds. (**C**) (i) In human dermal fibroblasts cultured for 5 days, incubation for 30 minutes with 200 nM fibulin-4 did not stimulate Smad2 phosphorylation. The presence of microfibril-associated latent TGFβ was confirmed by addition of the fibrillin-1 fragment PF10 (200 nM), which releases LTBP-1 from microfibrils and activates TGFβ (Chaudhry et al., 2007); in these samples (with or without fibulin-4), Smad2 phosphorylation was detected. Exogenous TGFβ1 (4 nM) is shown as positive control, and no protein added (untreated) as negative control. One representative experiment is shown. (ii) Graphic representation of the Smad2-phosphorylation gel data, with or without added fibulin-4, PF10 or exogenous TGFβ1. Quantitative analysis was performed by densitometry with data normalized against β-actin. Data are represented as the mean ± s.e.m. of three experiments. *P<0.05; ***P<0.0001.

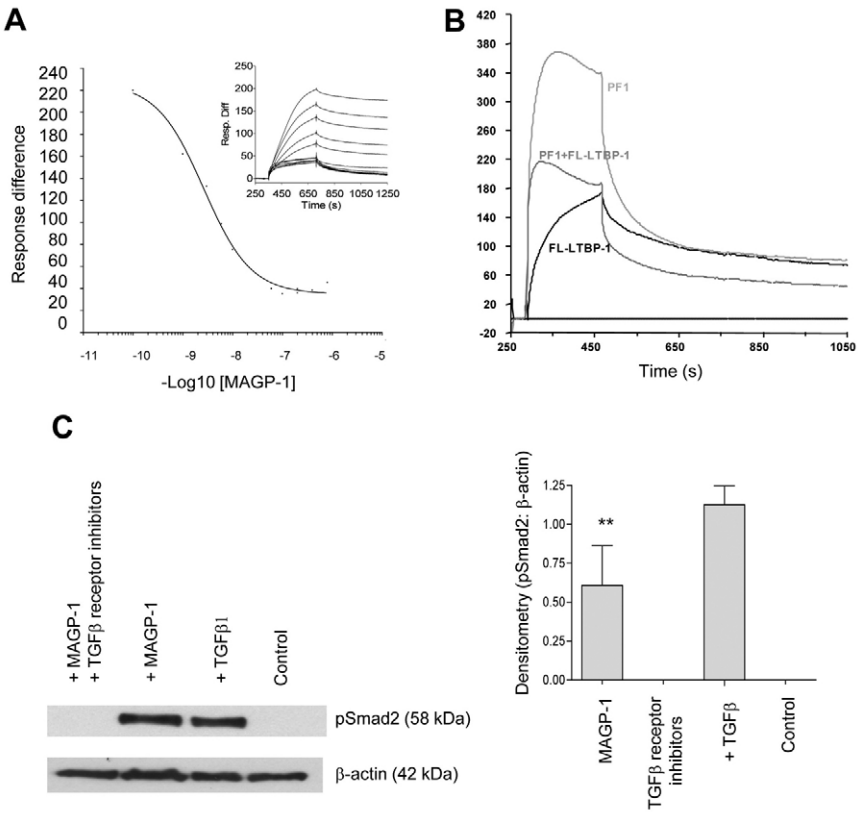

Fig. 9. MAGP-1 inhibits LTBP-1 binding to fibrillin-1 and induces Smad2 phosphorylation. (**A**) BIAcore analysis of the binding of C-terminal LTBP-1, immobilized on a CM5 chip, to the fibrillin-1 $PF1^{Ex5-7}$ fragment revealed that MAGP-1 (0-800 nM) strongly inhibited the C-terminal LTBP-1 interaction with 200 nM fibrillin-1 $PF1^{Ex5-7}$ (EC_{50}=2.63 nM). One representative experiment is shown. Response difference is the difference between experimental and control flow cells in response units. Inhibition curves were plotted using the response values of each normalized curve at the end of the association period. (**B**) BIAcore analysis of the binding of PF1 and/or full-length LTBP-1 to immobilized monomeric MAGP-1. Pre-incubation with full-length LTBP-1 reduced PF1 binding to MAGP-1. (**C**) MAGP-1 (500 nM) stimulated TGFβ-receptor-dependent Smad2 phosphorylation in human dermal fibroblasts, after incubation for 15 minutes (**P<0.05 Student's t-test) (blot and graph). By contrast, TGFβ receptor (TGFβR) I and II inhibitor-treated controls, or negative controls with no protein added showed no Smad2 phosphorylation. Quantitative analysis (graph) was performed by densitometry with data normalized against β-actin. Data are represented as the mean ± s.e.m. of three experiments.

4 inhibits full-length and C-terminal LTBP-1 from binding to PF1 (not shown), which agrees with the findings of Ono et al. (Ono et al., 2009). In addition, microfibril-associated molecules MAGP-1 (Fig. 8Bi) and heparin (Fig. 8Bii) both partially reduced binding of full-length LTBP-1 to immobilized full-length fibulin-4. Taken together, the data show that fibulin-4 is a crucial mediator of the association of LTBP-1 with microfibrils.

When fibroblasts were incubated with fibulin-4, no Smad2 phosphorylation was induced (Fig. 8C). Using the fibrillin-1 fragment PF10, which we have previously shown to displace LTBP-1 from fibrillin-1 thereby activating TGFβ by releasing it from microfibrils (Chaudhry et al., 2007), we confirmed that microfibril-associated latent TGFβ was indeed present in these cultures.

MAGP-1 inhibits LTBP-1 binding to fibrillin-1

MAGP-1 is a microfibril-associated component that binds an N-terminal sequence of fibrillin-1 adjacent to the convertase-cleavage site (Jensen et al., 2001; Cain et al., 2008). Although it is not essential for microfibril assembly, *MAGP-1*-null mice have phenotypic traits consistent with loss of TGFβ function (Weinbaum et al., 2008). BIAcore analysis revealed that MAGP-1 did not bind immobilized full-length LTBP-1 (not shown). However, MAGP-1 strongly inhibited the C-terminal LTBP-1 interaction with fibrillin-1 PF1 [effector concentration for half-maximum response (EC_{50})=198.7 nM] (not shown) and $PF1^{Ex5-7}$ (EC_{50}=2.63 nM) (Fig. 9A), and the interaction between MAGP-1 and fibrillin-1 (PF1) was also reduced by full-length LTBP-1 (Fig. 9B). Thus, the binding of MAGP-1 and LTBP-1 to fibrillin-1 might be mutually exclusive. Furthermore, MAGP-1 strongly stimulated TGFβ-receptor-dependent Smad2 phosphorylation in human dermal fibroblasts after incubation with MAGP-1 for 15 minutes (Fig. 9C). We confirmed by TGFβ1 ELISA and immunoblotting that the purified MAGP-1 preparations contained virtually no detectable TGFβ (<10 pg/ml) (not shown). Thus, MAGP-1 can release LTBP-1 from assembled microfibrils, thereby enhancing TGFβ activity.

In summary, our data show that LTBP-1 and/or LLC deposition is dependent on microfibril assembly. The association of LTBP-1 with newly synthesized fibrillin-1 is governed by pericellular heparan sulfate. Fibulin-4 seems to be a crucial mediator of the association of LTBP-1 and/or LLC with microfibrils, but MAGP-1 disrupts these interactions. In this way, microfibrils regulate TGFβ bioavailability.

Discussion

The importance of fibrillin microfibrils for extracellular storage of latent TGFβ has been demonstrated in disease and in mouse models (Ramirez and Rifkin, 2009). However, the mechanism of LLC sequestration within the extracellular matrix and its subsequent release and TGFβ activation are poorly understood. It was proposed that LTBP-1 associates with fibronectin (Taipale et al., 1996; Vehviläinen et al., 2009) and subsequently relocates to fibrillin microfibrils (Ramirez and Rifkin, 2009); although there is no evidence for how this translocation may occur, it has been shown that fibronectin dimers can form higher-order assemblies in non-covalent association with fibrillin microfibrils (Ohashi and Erickson, 2009). Our data indicate that LTBP-1 associates with fibrillin during the assembly of microfibrils, and that LTBP-1-associated microfibrils colocalize with fibronectin during the formation of higher-order networks. It has not been known whether LLC binds fibrillin prior, during or after microfibril assembly, or whether microfibril-associated molecules influence this association.

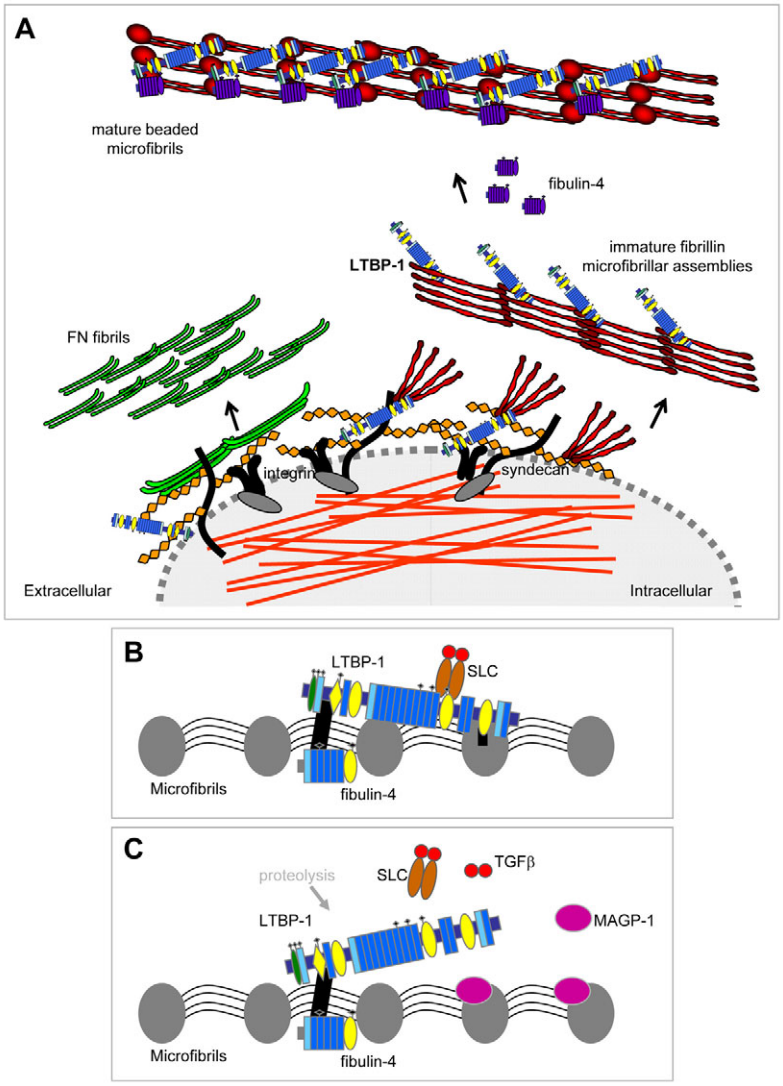

Fig. 10. Model of the LTBP-1 association with fibrillin microfibrils. (**A**) Model of how the pericellular environment, especially heparan-sulfate proteoglycans such as syndecans, facilitates transient colocalization of LTBP-1 with fibronectin, and the association of LTBP-1 with fibrillin-1 during pericellular microfibril assembly. (**B**) Schematic model showing LTBP-1 binding through its C-terminal region to fibrillin microfibrils, and how fibulin-4 interactions with N-terminal LTBP-1 stabilize this interaction. Thick black lines indicate molecular interactions. (**C**) Schematic model of how MAGP-1 can dislodge C-terminal LTBP-1 from microfibrils, thereby releasing TGFβ. N-terminal crosslinked LTBP-1 might be released from microfibrils after proteolysis (Hyytiäinen et al., 2004). Thick black lines indicate molecular interactions. Active TGFβ is indicated by red circles.

Our experiments shed crucial light on these key issues (Fig. 10). We have discovered that LTBP-1 and/or LLC deposition is dependent on receptor-mediated microfibril assembly and that, whereas full-length LTBP-1 binds only weakly to newly secreted pro-fibrillin-1, this association is governed by pericellular heparan sulfate and microfibril-associated molecules.

Immunofluorescence analysis showed fine punctate LTBP-1 filaments assembling along the cell surface, and that LTBP-1 and fibrillin-1 colocalized within the same fibrillar networks. These assemblies were reminiscent of cell-surface LTBP-1 in an earlier scanning-EM study (Taipale et al., 1996). Although both fibrillin-1 and LTBP-1 partially colocalized with fibronectin, exogenous heparin blocked deposition of both LTBP-1 and microfibrils, but not fibronectin; this deposition was most probably blocked by heparin directly competing with heparan-sulfate-dependent fibrillin-1 terminal assembly interactions (Cain et al., 2008) and interactions with syndecans (Bax et al., 2007). Exogenous heparin might also compete with other matrix interactions that depend on cell-surface heparan sulphate. Inhibiting α5β1 integrin blocked deposition of LTBP-1, as well as of microfibrils as reported (Kinsey et al., 2008), so deposition of LTBP-1 either requires receptor-mediated fibrillin assembly or associates independently with matrix in an α5β1-integrin-dependent manner. Stable knockdown of fibrillin-1, which dramatically reduced LTBP-1 and LLC deposition in matrix, confirmed the requirement for fibrillin-1. Fibrillin-2, which, similar to fibrillin-1, can bind LTBP-1 through an N-terminal region (Isogai et al., 2003), also supported fibrillar LTBP-1 deposition.

Although C-terminal LTBP-1 binds strongly to N-terminal fibrillin-1, we found that full-length LTBP-1 bound only weakly to fibrillin-1, indicating that the fibrillin-1-binding site is masked in full-length LTBP-1. Nevertheless, LTBP-1 colocalized and co-immunoprecipitated with fibrillin-1, so they do associate. We have found that the association of LTBP-1 with newly synthesized fibrillin-1 is governed by pericellular heparan sulfate, which can bind both molecules. It seems likely that endogenous heparan sulfate brings these molecules together at the cell surface during microfibril assembly. The data suggest that the conformation of purified native full-length LTBP-1 in the absence of heparan sulfate impedes fibrillin-1 binding to its C-terminal region (Fig. 10). We speculate that it might also preclude binding to fibronectin, providing an explanation for apparently conflicting data (Fontana et al., 2005; Chen et al., 2007).

Deciphering the binding site for LTBP-1 on N-terminal fibrillin-1 has proved difficult. Previously it was shown that C-terminal LTBP-1 binds four N-terminal fibrillin-1 domains (EGF2, EGF3, first hybrid and cbEGF1) and weakly to the two EGFs preceding the

first hybrid domain, and that deletion or disruption of the first hybrid domain reduced affinity for C-terminal LTBP-1 (Isogai et al., 2003; Ono et al., 2009). Here we have shown that C-terminal LTBP-1 binds well to the first hybrid domain and subsequent cbEGF domain, that the EGF preceding the first hybrid domain influences this interaction, and that the $PF1^{Ex5-7}$ subfragment binds more strongly than does PF1 itself. These data further indicate that the fibrillin-1-binding region for LTBP-1 must be conformation-dependent.

We have found that MAGP-1 can strongly inhibit LTBP-1 binding to N-terminal fibrillin-1, thereby enhancing active TGFβ, so its role might be to fine-tune levels of LLC associated with microfibrils (Fig. 10). Thus, in *MAGP-1*-null mice (Weinbaum et al., 2008), lack of competition for LLC binding to microfibrils could result in enhanced microfibril-bound LLC and reduced active TGFβ. By contrast, enhanced TGFβ activity in mice depleted of fibulin-4 (Hanada et al., 2007) suggests a stabilizing role for fibulin-4, which is consistent with our finding that, unlike MAGP-1, exogenous fibulin-4 does not release TGFβ from microfibrils. We have also shown that fibulin-4 can strongly bind LTBP-1, and can simultaneously bind LTBP-1 and fibrillin-1, implicating fibulin-4 as a key mediator in the association of LTBP-1 with microfibrils (Fig. 10). The severe elastic fibre phenotype of fibulin-4-depleted mice might thus reflect not only perturbed elastin crosslinking (Horiguchi et al., 2009), but also altered release of LLC from microfibrils. One N-terminal fibrillin-1 Marfan mutant exhibited significantly reduced LTBP-1 binding to fibrillin-1; this binding might also contribute to this pathology.

In summary, we have shown that LTBP-1 and/or LLC deposition is dependent on pericellular microfibril assembly and governed by complex interactions between LTBP-1, cell-surface heparan sulfate, microfibril-associated molecules and fibronectin. In this way, microfibrils control TGFβ bioavailability.

Materials and Methods

Cell culture

Tissue-culture reagents were purchased from Sigma-Aldrich (Dorset, UK). Human dermal fibroblasts were purchased from Invitrogen (Glasgow, UK). 293-EBNA cells were purchased from the American Type Tissue Culture Collection. ARPE-19 cells were obtained from the American Tissue Culture Collection. Cells were routinely maintained in Dulbecco's Modified Eagle's Medium (DMEM) supplemented with 10% fetal calf serum, 1% L-glutamine and 100 U/ml penicillin/streptomycin at 37°C in 5% CO_2.

Expression and purification of recombinant fibrillin-1 fragments

Recombinant human fibrillin-1 PF1 and subfragments, and PF13 were expressed in 293-EBNA cells using the pCEP-His vector, as described (Rock et al., 2004; Cain et al., 2005; Chaudhry et al., 2007; Cain et al., 2008) (Fig. 1A). Subfragments $PF1^{Ex5-7}$ and $PF1^{Ex6,7}$ were generated as described (Cain et al., 2008).

For N-terminal fibrillin-1 Marfan syndrome mutants, single-point mutations were engineered into wild-type PF1 using site-directed mutagenesis. Oligonucleotide primers for mutagenesis were synthesized by Eurofins MWG Operon (Germany). The primers were (5′-3′): R62C forward primer: GTCTGTGGATCATGTTATAATGCTTACTGTTGCCC; reverse primer: GGGCAACAGTAAGCATTATAACATGATCCACAGAC; S115C forward primer: CCTGTGGCTCCAGATGCATACAACACTGC; reverse primer: GCAGTGTTGTATGCATCTGGAGCCACAGG; T101A forward primer: GCCAAATATGTGCGCTTGCCCATCTGGTCAG; reverse primer: CTGACCAGATGGGCAAGCGCACATATTTGGC; C129Y forward primer: GAGGTAGCTACAGTGACGATCACTG; reverse primer: CAGTGATCGTCACTGTAGCTACCTC; C166S forward primer: CCCCAAATCGAAGTGCATGCACTTACG; reverse primer: CGTAAGTGCATGCACTTCGATTTGGGG; R240C forward primer: GCTTCATTCCAAATATCTGCACGGGAGCTTG, reverse primer: CAAGCTCCCGTGCAGATATTTGGAATGAAGC; E383L forward primer: GCTTCATTCCAAATATCTGCACGGGAGCTTG; reverse primer: CAAGCTCCCGTGCAGATATTTGGAATGAAGC; V449I forward primer: GGGTGCTGCCAGTAAACATTACTGATTACTGCC; reverse primer: GGCAGTAATCAGTAATGTTTACTGGCAGCACCC.

DNA sequencing confirmed that all sequences were correct. All proteins were purified by nickel chromatography, monomers were isolated by gel filtration chromatography in 150 mM NaCl, 0.5 mM $CaCl_2$, 5 mM HEPES, pH 7.4, and monomeric status was confirmed by multi-angle laser light scattering (Cain et al., 2008; Choudhury et al., 2009). Purified recombinant PF1 (Cain et al., 2008), $PF1^{Ex6+7}$ and $PF1^{Ex5-7}$ (Fig. 1C) migrated on SDS-PAGE gels with predicted molecular masses of 53 kDa, 16 kDa and 24 kDa, respectively. The PF1 mutant fragments all had the predicted mass of 53 kDa (not shown). All fragments with predicted N-glycosylation sites were shown to be glycosylated, using N-glycosidase F (PNGase F), as described (Rock et al., 2004; Cain et al., 2005).

Expression and purification of recombinant LTBP-1

Human LTBP-1S clones were obtained from Sarah L. Dallas (University of Missouri, Kansas City, KS). Recombinant full-length human LTBP-1 and a C-terminal fragment of LTBP-1 were expressed in 293-EBNA cells using pCEP-His, and purified as described (Chaudhry et al., 2007) (Fig. 1C). By SDS-PAGE analysis plus 10 mM dithiothreitol, the relative molecular mass (M_r) of full-length LTBP-1 and C-terminal LTBP-1 were ~170 kDa and 52 kDa, respectively. The presence of N-linked sugars was confirmed using N-glycosidase F (PNGase F) digestions.

Expression and purification of recombinant MAGP-1 and fibulin-4

Recombinant human full-length MAGP-1, full-length fibulin-4, and N- and C-terminal halves of fibulin-4, were expressed in 293-EBNA cells using pCEP-His, and monomers purified as previously described (Rock et al., 2004; Choudhury et al., 2009). Because MAGP-1 can bind TGFβ (Weinbaum et al., 2008), we confirmed by immunoblotting that purified recombinant monomeric MAGP-1 did not contain TGFβ, using anti-TGFβ1 mAb (mAb240, R&D Systems) (not shown). The TGFβ1 E_{max} ImmunoAssay System (Promega) confirmed <10 pg/ml TGFβ1 present in recombinant MAGP-1 preparations (not shown).

Smad2 phosphorylation assays

Smad2 phosphorylation assays were conducted as described (Chaudhry et al., 2007). For function-blocking assays, cells were treated with 20 μg/ml inhibitory integrin antibodies α5 (mAb16) and β1 (mAb13) (gift from Martin J. Humphries, University of Manchester, Manchester, UK). For TGFβ-receptor-inhibition assays, inhibitors of TGFβ receptor I {[3-(pyridine-2-yl)-4-4-quinonyl)]-1 H-pyrazole (Merck Biosciences)} and TGFβ receptor II (anti-human antibody AF-241-NA; R&D Systems) were used at concentrations of 20 and 15 μg/ml, respectively. Cells were incubated at 37°C for 15 minutes in 0.5 ml serum-free DMEM with 3 μM recombinant fibrillin-1 (PF10) or fibulin-4 (200 nM) or MAGP-1 (500 nM). Recombinant human TGFβ1 was used as a positive control (4 nM) (Sigma-Aldrich, Dorset, UK). Western blots using an anti-Smad2 antibody (Ab3849; Chemicon Europe, Hampshire, UK) were developed using enhanced chemiluminescence (ECL) [GE Healthcare, Buckinghamshire, UK or SuperSignal (Pierce, UK)], and re-probed with β-actin (AC-15; Sigma-Aldrich, Dorset, UK) to ensure equal protein loadings. Densitometry was used for quantitative analysis, with data normalized against β-actin. Data are represented as the mean of repeated experiments and were statistically analyzed using ANOVA and unpaired Student's *t*-tests. The error bars represent the s.d. of the three experiments. Results are statistically significant when the *P* value is <0.05 (**P*<0.05, ***P*<0.001, ****P*<0.0001).

Co-immunoprecipitations

Human dermal fibroblasts and ARPE-19 cells at days 1-7 after plating were washed three times with phosphate-buffered saline (PBS), incubated with NET buffer supplemented with fresh proteinase inhibitors (as above) for 30 minutes, and scraped from the tissue-culture flask. Cell lysates were pre-cleared with protein-A Sepharose (GE Healthcare, UK) for 60 minutes with rotation. An anti-LTBP-1 monoclonal antibody (mAb388; R&D Systems) (Chen et al., 2007) was pre-incubated with protein-A–Sepharose beads, added to conditioned media and cell lysates overnight at 4°C prior to centrifugation at 800 ***g*** for 3 minutes, and pellets washed thrice in NET buffer. Immunoprecipitates were analyzed by SDS-PAGE and immunoblotting using anti-fibrillin-1 polyclonal antibody (from Penny A. Handford, Oxford, UK) and anti-LTBP-1 mAb (mAb388). Blots were developed using enhanced ECL (GE Healthcare, UK) and Kodak BioMax MR film.

Stable and transient knockdowns of fibrillin-1

Stable knockdown of fibrillin-1 in ARPE-19 cells was achieved using shRNA retroviral vector pSuper.retro.neo+gfp (pSR) (Oligoengine) (Fig. 3A, not shown). The vectors pVPack-GP and pVPack-VSV-G (Stratagene) were co-transfected along with pSR (containing either target fibrillin-1 RNAi sequence 5′-GCAAATGTCCCGTGGGATATG-3′ or a scrambled control) into 293T cells, resulting in retrovirus production. Viral-containing media was used to transduce target ARPE-19 cells, and transduced cells were selected using geneticin. Knockdown was confirmed at mRNA (RT-PCR and quantitative PCR; 84% knockdown) and protein levels, and by immunofluorescence microscopy (Fig. 3B; not shown). RNA interference of fibrillin-1 and fibrillin-2 was also performed (not shown).

Immunofluorescence microscopy

Adult human dermal fibroblasts and ARPE-19 cells were immunostained, essentially as described (Kinsey et al., 2008). Briefly, cells were cultured for up to 14 days, without or with 0.5 mg/ml heparin (Iduron, Manchester, UK), or 10 μg/ml mAbs that inhibit α5, β1, αv and αvβ3 integrins [mAb16, mAb13, mAb 17E6 (Calbiochem,

UK), and mAb LM609 (Millipore, UK), respectively], or non-function-blocking α5 integrin mAb11, with mouse IgG as control; media and supplements were replaced every 2 days (Kinsey et al., 2008). Fixed permeabilized cells were incubated with rabbit anti-human fibrillin-1 (proline-region) polyclonal antibody (1:400) (Kinsey et al., 2008), or anti-human LTBP-1 mAb (1:300 of 1 mg/ml stock; mAb388, clone 35409, R&D Systems, USA), or anti-human fibrillin-2 polyclonal antibody (1:50; N-20, Santa Cruz Biotechnology), or anti-fibronectin (3E2 mAb to cellular fibronectin), in PBS containing 3% (w/v) fish skin gelatin. For triple staining, we used sheep anti-human fibronectin polyclonal antibody (1:1500 of 0.2 mg/ml stock; AF1918, R&D Systems) with Alexa-Fluor-647 donkey anti-sheep (Invitrogen). Secondary antibodies were Alexa-Fluor-594 donkey anti-rabbit or anti-goat IgG (H+L) and Alexa-Fluor-488 donkey anti-mouse IgG (H+L) (Invitrogen, UK). Cells were mounted onto microscope slides with DAPI (Vector Laboratories, UK).

Images were collected on a wide-field upright microscope (Olympus BX51) using 20× and 60× objectives and captured using a CoolSNAP EZ camera (Photometrics) driven by MetaVue Software (Molecular Devices). Specific band-pass filter sets for DAPI, FITC and Texas Red, and Cy5 (Alexa Fluor 647) for triple-staining experiments, were used to prevent bleed-through. Images were processed and analyzed using ImageJ software. Images of ARPE-19 fibrillin-1 knockdown cells were collected using a Nikon C1 confocal on an upright 90i microscope with 60×/1.40 Plan Apo objective. The confocal settings were: pinhole 30 µm, scan speed 400 Hz unidirectional, format 512×512. Images for DAPI, FITC and Texas Red were excited with the 405 nm, 488 nm and 543 nm laser lines, respectively. When it was not possible to eliminate cross-talk between channels, images were collected sequentially. When acquiring 3D optical stacks, the confocal software was used to determine the optimal number of *z* sections. Only maximum intensity projections of the 3D stacks are shown in the Results.

Rotary shadowing electron microscopy

Samples were prepared for shadowing using a modified version of the mica sandwich technique (Mould et al., 1985) in the presence or absence of heparin. Samples on mica were shadowed using a Cressington CFE-60 freeze fracture/etch unit. Carbon-coated grids were viewed on an FEI Tecnai Biotwin transmission electron microscope operated at 100 kV, and images were recorded at 23k or 30k on a Gatan Orius SC1000 digital camera.

Solid-phase-binding assays

Solid-phase binding, using biotinylated soluble ligands, was performed as described (Choudhury et al., 2009). All assays were performed in triplicate and repeated at least twice.

BIAcore 3000 analysis

Surface plasmon resonance using a BIAcore biosensor was used to perform kinetic binding and inhibition analyses of fibrillin-1, LTBP-1, MAGP-1, fibulin-4 and heparin (dp20; Iduron, Manchester, UK) (BIAcore 3000, BIAcore AB, Sweden; http://www.biacore.com/lifesciences). For further information, see Jason-Moller et al. (Jason-Moller et al., 2006) and Piliarik et al. (Piliarik et al., 2009). Full-length or C-terminal LTBP-1 was immobilized onto a CM5 sensor chip at 10 µg/ml or 25 µg/ml in 50 mM sodium acetate buffer, pH 4.0 or 3.0, respectively. Fibrillin-1 fragments PF1 and $PF1^{Ex5\text{-}7}$ or $PF1^{Ex6+7}$ (0-1000 nM) were applied to a coated sensor chip (20 µl/min) for 6 minutes and then left to dissociate for 10 minutes. Regeneration was performed in 10 mM HEPES, pH 7.4, 0.4 M NaCl, 1 mM $CaCl_2$ and 0.005% Tween 20. The K_D values for the fibrillin-1 interactions were calculated by plotting saturation binding curves using the equilibrium response value at the top of the curve, as described (Cain et al., 2005). All assays were performed at least twice; final K_D values were calculated from an average of these values.

Similar binding studies were conducted in triplicate, using immobilized full-length LTBP-1 and soluble fibulin-4 (2, 4, 6, 8, 10 µg/ml), or immobilized full-length fibulin-4 and soluble full-length LTBP-1 (2, 4, 6, 8, 10 µg/ml), with or without pre-incubation with PF1 (0-1000 nM) or MAGP-1 (0-1000 nM). Binding-inhibition studies were also conducted using immobilized LTBP-1 and soluble $PF1^{Ex5\text{-}7}$ (0-1000 nM) or fibulin-4 (0-1000 nM). Heparin (3000 Da; Sigma Aldrich, UK) (0-3000 nM) was pre-incubated with PF1, $PF1^{Ex1\text{-}11}$ or $PF1^{Ex5\text{-}7}$ (all at 200 nM) for 10 minutes prior to injecting across immobilized LTBP-1, to determine whether heparin altered PF1 binding to immobilized full-length LTBP-1.

This study was funded by the Medical Research Council (UK). We are grateful to Stuart Cain for preparing recombinant human MAGP-1 and PF1 fragments and to Roger Meadows for assistance with rotary shadowing EM. Deposited in PMC for release after 6 months.

References

Bax, D. V., Mahalingam, Y., Cain, S., Mellody, K., Freeman, L., Younger, K., Shuttleworth, C. A., Humphries, M. J., Couchman, J. R. and Kielty, C. M. (2007). Cell adhesion to fibrillin-1: identification of an Arg-Gly-Asp-dependent synergy region and a heparin-binding site that regulates focal adhesion formation. *J. Cell Sci.* **120**, 1383-1392.

Biggin, A., Holman, K., Brett, M., Bennetts, B. and Adès, L. (2004). Detection of thirty novel FBN1 mutations in patients with Marfan syndrome or a related fibrillinopathy. *Hum. Mutat.* **23**, 99.

Cain, S. A., Baldock, C., Gallagher, J., Morgan, A., Bax, D. V., Weiss, A. S., Shuttleworth, C. A. and Kielty, C. M. (2005). Fibrillin-1 interactions with heparin. Implications for microfibril and elastic fiber assembly. *J. Biol. Chem.* **280**, 30526-30537.

Cain, S. A., Morgan, A., Sherratt, M. J., Ball, S. G., Shuttleworth, C. A. and Kielty, C. M. (2006). Proteomic analysis of fibrillin-rich microfibrils. *Proteomics* **6**, 111-122.

Cain, S. A., Baldwin, A. K., Mahalingam, Y., Raynal, B., Jowitt, T. A., Shuttleworth, C. A., Couchman, J. R. and Kielty, C. M. (2008). Heparan sulfate regulates fibrillin-1 N- and C-terminal interactions. *J. Biol. Chem.* **283**, 27017-27027.

Chaudhry, S. S., Cain, S. A., Morgan, A., Dallas, S. L., Shuttleworth, C. A. and Kielty, C. M. (2007). Fibrillin-1 regulates the bioavailability of TGFbeta1. *J. Cell Biol.* **176**, 355-367.

Chen, Q., Sivakumar, P., Barley, C., Peters, D. M., Gomes, R. R., Farach-Carson, M. C. and Dallas, S. L. (2007). Potential role for heparan sulfate proteoglycans in regulation of transforming growth factor-beta (TGF-beta) by modulating assembly of latent TGF-beta-binding protein-1. *J. Biol. Chem.* **282**, 26418-26430.

Choudhury, R., McGovern, A., Ridley, C., Cain, S. A., Baldwin, A., Wang, M. C., Guo, C., Mironov, A., Jr, Drymoussi, Z., Trump, D. et al. (2009). Differential regulation of elastic fiber formation by fibulin-4 and -5. *J. Biol. Chem.* **284**, 24553-24567.

Comeglio, P., Evans, A. L., Brice, G., Cooling, R. J. and Child, A. H. (2002). Identification of FBN1 gene mutations in patients with ectopia lentis and marfanoid habitus. *Br. J. Ophthalmol.* **86**, 1359-1362.

Dallas, S. L., Keene, D. R., Bruder, S. P., Saharinen, J., Sakai, L. Y., Mundy, G. R. and Bonewald, L. F. (2000). Role of the latent transforming growth factor beta binding protein 1 in fibrillin-containing microfibrils in bone cells in vitro and in vivo. *J. Bone Miner. Res.* **15**, 68-81.

Dallas, S. L., Rosser, J. L., Mundy, G. R. and Bonewald, L. F. (2002). Proteolysis of latent transforming growth factor-beta (TGF-beta)-binding protein-1 by osteoclasts. A cellular mechanism for release of TGF-beta from bone matrix. *J. Biol. Chem.* **277**, 21352-21360.

Dallas, S. L., Sivakumar, P., Jones, C. J., Chen, Q., Peters, D. M., Mosher, D. F., Humphries, M. J. and Kielty, C. M. (2005). Fibronectin regulates latent transforming growth factor-beta (TGF beta) by controlling matrix assembly of latent TGF beta-binding protein-1. *J. Biol. Chem.* **280**, 18871-18880.

Fontana, L., Chen, Y., Prijatelj, P., Sakai, T., Fässler, R., Sakai, L. Y., Rifkin, D. B. (2005). Fibronectin is required for integrin alphavbeta6-mediated activation of latent TGF-beta complexes containing LTBP-1. *FASEB J.* **19**, 1798-1808.

Ge, G. and Greenspan, D. S. (2006). BMP1 controls TGFbeta1 activation via cleavage of latent TGFbeta-binding protein. *J. Cell Biol.* **175**, 111-120.

Hanada, K., Vermeij, M., Garinis, G. A., de Waard, M. C., Kunen, M. G., Myers, L., Maas, A., Duncker, D. J., Meijers, C., Dietz, H. C. et al. (2007). Perturbations of vascular homeostasis and aortic valve abnormalities in fibulin-4 deficient mice. *Circ. Res.* **100**, 738-746.

Horiguchi, M., Inoue, T., Ohbayashi, T., Hirai, M., Noda, K., Marmorstein, L. Y., Yabe, D., Takagi, K., Akama, T. O., Kita, T. et al. (2009). Fibulin-4 conducts proper elastogenesis via interaction with cross-linking enzyme lysyl oxidase. *Proc. Natl. Acad. Sci. USA* **106**, 19029-19034.

Hubmacher, D., El-Hallous, E. I., Nelea, V., Kaartinen, M. T., Lee, E. R. and Reinhardt, D. P. (2008). Biogenesis of extracellular microfibrils: Multimerization of the fibrillin-1 C terminus into bead-like structures enables self-assembly. *Proc. Natl. Acad. Sci. USA* **105**, 6548-6553.

Hyytiäinen, M., Penttinen, C. and Keski-Oja, J. (2004). Latent TGF-beta binding proteins: extracellular matrix association and roles in TGF-beta activation. *Crit. Rev. Clin. Lab. Sci.* **41**, 233-264.

Isogai, Z., Ono, R. N., Ushiro, S., Keene, D. R., Chen, Y., Mazzieri, R., Charbonneau, N. L., Reinhardt, D. P., Rifkin, D. B. and Sakai, L. Y. (2003). Latent transforming growth factor beta-binding protein 1 interacts with fibrillin and is a microfibril-associated protein. *J. Biol. Chem.* **278**, 2750-2757.

Jason-Moller, L., Murphy, M. and Bruno, J. (2006). Overview of Biacore systems and their applications. *Curr. Protoc. Protein Sci.* **Chp. 19**, 19.13.

Jensen, S. A., Reinhardt, D. P., Gibson, M. A. and Weiss, A. S. (2001). Protein interaction studies of MAGP-1 with tropoelastin and fibrillin-1. *J. Biol. Chem.* **276**, 39661-39666.

Kinsey, R., Williamson, M. R., Chaudhry, S., Mellody, K. T., McGovern, A., Takahashi, S., Shuttleworth, C. A. and Kielty, C. M. (2008). Fibrillin-1 microfibril deposition is dependent on fibronectin assembly. *J. Cell Sci.* **121**, 2696-2704.

Kobayashi, N., Kostka, G., Garbe, J. H., Keene, D. R., Bächinger, H. P., Hanisch, F. G., Markova, D., Tsuda, T., Timpl, R., Chu, M. L. et al. (2007). A comparative analysis of the fibulin protein family. Biochemical characterization, binding interactions, and tissue localization. *J. Biol. Chem.* **282**, 11805-11816.

Marson, A., Rock, M. J., Cain, S. A., Freeman, L. J., Morgan, A., Mellody, K., Shuttleworth, C. A., Baldock, C. and Kielty, C. M. (2005). Homotypic fibrillin-1 interactions in microfibril assembly. *J. Biol. Chem.* **280**, 5013-5021.

McLaughlin, P. J., Chen, Q., Horiguchi, M., Starcher, B. C., Stanton, J. B., Broekelmann, T. J., Marmorstein, A. D., McKay, B., Mecham, R., Nakamura, T. et al. (2006). Targeted disruption of fibulin-4 abolishes elastogenesis and causes perinatal lethality in mice. *Mol. Cell. Biol.* **26**, 1700-1709.

Miyazono, K., Olofsson, A., Colosetti, P. and Heldin, C. H. (1991). A role of the latent TGF-beta 1-binding protein in the assembly and secretion of TGF-beta 1. *EMBO J.* **10**, 1091-1101.

Mould, A. P., Holmes, D. F., Kadler, K. E. and Chapman, J. A. (1985). Mica sandwich technique for preparing macromolecules for rotary shadowing. *J. Ultrastruct. Res*. **91**, 66-76.

Munger, J. S., Harpel, J. G., Gleizes, P. E., Mazzieri, R., Nunes, I. and Rifkin, D. B. (1997). Latent transforming growth factor-beta: structural features and mechanisms of activation. *Kidney Int.* **51**, 1376-1382.

Nunes, I., Gleizes, P. E., Metz, C. N. and Rifkin, D. B. (1997). Latent transforming growth factor-beta binding protein domains involved in activation and transglutaminase-dependent cross-linking of latent transforming growth factor-beta. *J. Cell Biol.* **136**, 1151-1163.

Ohashi, T. and Erickson, H. P. (2009). Revisiting the mystery of fibronectin multimers: the fibronectin matrix is composed of fibronectin dimers cross-linked by non-covalent bonds. *Matrix Biol.* **28**, 170-175.

Ono, R. N., Sengle, G., Charbonneau, N. L., Carlberg, V., Bächinger, H. P., Sasaki, T., Lee-Arteaga, S., Zilberberg, L., Rifkin, D. B., Ramirez, F. et al. (2009). Latent transforming growth factor beta-binding proteins and fibulins compete for fibrillin-1 and exhibit exquisite specificities in binding sites. *J. Biol. Chem*. **284**, 16872-16881.

Piliarik, M, Vaisocherová, H. and Homola, J. (2009). Surface plasmon resonance biosensing. *Methods Mol. Biol*. **503**, 65-88.

Qian, R. Q. and Glanville, R. W. (1997). Alignment of fibrillin molecules in elastic microfibrils is defined by transglutaminase-derived cross-links. *Biochemistry* **36**, 15841-15847.

Raghunath, M., Unsöld, C., Kubitscheck, U., Bruckner-Tuderman, L., Peters, R. and Meuli, M. (1998). The cutaneous microfibrillar apparatus contains latent transforming growth factor-beta binding protein-1 (LTBP-1) and is a repository for latent TGF-beta1. *J. Invest. Dermatol.* **111**, 559-564.

Ramirez, F. and Rifkin, D. B. (2009). Extracellular microfibrils: contextual platforms for TGFbeta and BMP signaling. *Curr. Opin. Cell Biol.* **21**, 616-622.

Ramirez, F. and Sakai, L. Y. (2010). Biogenesis and function of fibrillin assemblies. *Cell Tissue Res.* **339**, 71-82.

Ritty, T. M., Broekelmann, T. J., Werneck, C. C. and Mecham, R. P. (2003). Fibrillin-1 and -2 contain heparin-binding sites important for matrix deposition and that support cell attachment. *Biochem. J.* **375**, 425-432.

Robinson, P. N., Arteaga-Solis, E., Baldock, C., Collod-Béroud, G., Booms, P., De Paepe, A., Dietz, H. C., Guo, G., Handford, P. A., Judge, D. P. et al. (2006). The molecular genetics of Marfan syndrome and related disorders. *J. Med. Genet.* **43**, 769-787.

Rock, M. J., Cain, S. A., Freeman, L. J., Morgan, A., Mellody, K., Marson, A., Shuttleworth, C. A., Weiss, A. S. and Kielty, C. M. (2004). Molecular basis of elastic fiber formation. Critical interactions and a tropoelastin-fibrillin-1 cross-link. *J. Biol. Chem.* **279**, 23748-23758.

Sabatier, L., Chen, D., Fagotto-Kaufmann, C., Hubmacher, D., McKee, M. D., Annis, D. S., Mosher, D. F. and Reinhardt, D. P. (2009). Fibrillin assembly requires fibronectin. *Mol. Biol. Cell* **20**, 846-858.

Sato, F., Wachi, H., Ishida, M., Nonaka, R., Onoue, S., Urban, Z., Starcher, B. C. and Seyama, Y. (2007). Distinct steps of cross-linking, self-association, and maturation of tropoelastin are necessary for elastic fiber formation. *J. Mol. Biol.* **369**, 841-851.

Sinha, S., Heagerty, A. M., Shuttleworth, C. A. and Kielty, C. M. (2002). Expression of latent TGF-beta binding proteins and association with TGF-beta 1 and fibrillin-1 following arterial injury. *Cardiovasc. Res.* **53**, 971-983.

Taipale, J., Saharinen, J., Hedman, K. and Keski-Oja, J. (1996). Latent transforming growth factor-beta 1 and its binding protein are components of extracellular matrix microfibrils. *J. Histochem. Cytochem.* **44**, 875-889.

Tatti, O., Vehviläinen, P., Lehti, K. and Keski-Oja, J. (2008). MT1-MMP releases latent TGF-beta1 from endothelial cell extracellular matrix via proteolytic processing of LTBP-1. *Exp. Cell Res.* **314**, 2501-2514.

Telci, D. and Griffin, M. (2006). Tissue transglutaminase (TG2) – a wound response enzyme. *Front. Biosci.* **11**, 867-882.

Telci, D., Collighan, R. J., Basaga, H. and Griffin, M. (2009). Increased TG2 expression can result in induction of transforming growth factor beta1, causing increased synthesis and deposition of matrix proteins, which can be regulated by nitric oxide. *J. Biol. Chem.* **284**, 29547-29558.

Tiedemann, K, Bätge, B., Müller, P. K. and Reinhardt, D. P. (2001). Interactions of fibrillin-1 with heparin/heparan sulfate, implications for microfibrillar assembly. *J. Biol. Chem*. **276**, 36035-36042.

Vehviläinen, P., Hyytiäinen, M. and Keski-Oja, J. (2009). Matrix association of latent TGF-beta binding protein-2 (LTBP-2) is dependent on fibrillin-1. *J. Cell. Physiol.* **221**, 586-593.

Verderio, E., Gaudry, C., Gross, S., Smith, C., Downes, S. and Griffin, M. (1999). Regulation of cell surface tissue transglutaminase: effects on matrix storage of latent transforming growth factor-beta binding protein-1. *J. Histochem. Cytochem.* **47**, 1417-1432.

Wallis, D. D., Putnam, E. A., Cretoiu, J. S., Carmical, S. G., Cao, S. N., Thomas, G. and Milewicz, D. M. (2003). Profibrillin-1 maturation by human dermal fibroblasts: proteolytic processing and molecular chaperones. *J. Cell. Biochem.* **90**, 641-652.

Weinbaum, J. S., Broekelmann, T. J., Pierce, R. A., Werneck, C. C., Segade, F., Craft, C. S., Knutsen, R. H. and Mecham, R. P. (2008). Deficiency in microfibril-associated glycoprotein-1 leads to complex phenotypes in multiple organ systems. *J. Biol. Chem.* **283**, 25533-25543.